Applied Energy 138 (2015) 121–132

Contents lists available at ScienceDirect

Applied Energy

journal homepage: www.elsevier.com/locate/apenergy

Study of solar regenerated membrane desiccant system to control humidity and decrease energy consumption in office spaces

Khoudor Keniar, Kamel Ghali, Nesreen Ghaddar *

Mechanical Engineering Department, American University of Beirut, P.O. Box 11-0236, Beirut 1107-2020, Lebanon

HIGHLIGHTS

- A model of solar-regenerated liquid desiccant membrane system was developed.
- The model predicts the humidity removal capacity from the space.
- The model was experimentally validated.
- The system resulted in 10% decrease in indoor relative humidity in Beirut climate.
- The system payback period was about 7 years.

ARTICLE INFO

Article history:
Received 19 July 2014
Received in revised form 9 October 2014
Accepted 24 October 2014
Available online 12 November 2014

Keywords:
Humidity control
Desiccant membrane dehumidification
Desiccant flow in permeable pipe
Moisture transfer

ABSTRACT

This paper investigates the feasibility of using a solar regenerated liquid desiccant membrane system to remove humidity from an office space. While conventional vapor compression cycles dehumidify the air before supplying it to the indoor space, through using sub cool–reheat process, the proposed cycle absorbs the humidity directly from indoor space through the dehumidifier. The dehumidifier consists of a set of permeable vertical tubes placed in the indoor space with liquid desiccant flowing through them. Solar energy is used as the source of thermal energy required for the regeneration of the desiccant and sea water is used as heat sink to provide the cooling needs of the liquid desiccant.

A mathematical model of the membrane desiccant system was integrated with the internal space model and solar system model to predict the humidity removal capacity from the space at given dehumidification and heat sink temperatures and outdoor environmental conditions. Experiments were performed to validate the model results be comparing exit humidity and temperature of the exit air from the space.

The validated model was applied to a case study consisting of an internal office during the month of August in Beirut hot humid climate. A decrease of 10% in indoor relative humidity is observed when the system was used. The cost of the proposed system was compared to the cost of a conventional vapor compression cycle that provides the same indoor conditions. A payback period of 7 years and 8 month was estimated compared to the investment in the vapor compression cycle.

1. Introduction

The control of indoor humidity is of fundamental importance for thermal comfort of human beings, building material sustainability and energy consumption. Thermal comfort deals with regulating the thermal environment, which includes temperature and relative humidity along with air velocity, around humans. Extreme levels of relative humidity, whether it is high or low, can irritate people's comfort [1]. Not only does it affect people, inappropriate levels of humidity also affect the building structure [2]. Negative impact of elevated moisture levels on building material includes electrochemical corrosion, volume changes, and chemical deterioration [3].

In order to eliminate the preceding negative impacts of elevated moisture levels, indoor humidity should be controlled, either by conventional or non-conventional techniques. In humid climates, the humidity issues are a major contributor to energy inefficiency in HVAC devices. The high humidity of the outside air combined with ventilation requirement increases the latent load. Most conventional air-conditioning systems are not designed to independently control temperature and humidity. The conventional way

* Corresponding author. Tel.: +961 1350000x2513.
E-mail address: farah@aub.edu.lb (N. Ghaddar).

http://dx.doi.org/10.1016/j.apenergy.2014.10.071

Nomenclature

T	temperature (°C)
T_{room}	indoor room temperature (°C)
c	concentration of water per desiccant (kg_{H_2O}/kg_{CaCl_2})
c_p	specific heat (J/kg K)
h_c	heat convection coefficient (W/m^2 s)
h_m	mass convection coefficient (m/s)
$h_{solution}$	enthalpy of the liquid desiccant solution (J/kg)
r_o	external radius of the pipe (m)
r_i	internal radius of the pipe (m)
E	power input/output (W)
D	diffusion constant of vapor in the pipe wall material (m^2/s)
k	thermal conductivity (W/m K)
m	mass rate (kg/s)
n	number of dehumidification/regeneration pipes
l	length of the pipe (m)
h_{fg}	latent heat of vaporization of the water (J/kg)
U	resistance coefficient per unit length
Q	internal heat generation (W)
Le	Lewis number

Greek letters

ρ	density (kg/m^3)
ω	humidity ratio (kg_{H_2O}/kg_{dryair})
$\omega^*_{solution}$	the equilibrium humidity ratio at surface of solution at temperature and concentration of solution (kg_{H_2O}/kg_{dryair})

Subscripts

solution	$CaCl_2$ and H_2O solution in the permeable tubes
o	outer side of the permeable tube
i	internal side of the permeable tube
inlet	inlet conditions to the space
outlet	outlet conditions to the space
m	mass convection
c	heat convection
a	air
v	water vapor
w	liquid water
d	desiccant $CaCl_2$
g	vapor generation

of moisture removal is cooling the indoor air (using vapor compression cycle) to temperatures below its dew point temperature to condense the excess moisture followed by reheating to the adequate supply air temperature. This is an energy intensive process [4,5]. Recently, research has been oriented towards considering non-conventional, passive and less-intensive methods for controlling indoor humidity. A known sustainable dehumidification technique is the use of desiccant technology as an active\passive method for HVAC applications [6–11].

Conventional desiccant dehumidification techniques utilize solid or liquid desiccant based systems. In the case when a liquid desiccant is used, dehumidification and regeneration tower beds are employed [6,9], whereas in the case of a solid desiccant, a rotary desiccant wheel is used [10]. An attractive feature of desiccant dehumidification systems is their suitability for solar or other low-grade thermal energy applications [6,7]. However, dehumidification of air is traditionally done through direct contact between the strong desiccant solution and the supply air. After the air is dehumidified, it is further cooled to the supply room temperature [9]. This technology can have many negative impacts related to health issues and corrosion problems especially with the entrainment of hazardous salts to the ventilation system due to the direct contact of air with the desiccant material [12].

To overcome the previous problems, researchers have recently implemented hydrophobic membranes to cool and dehumidify the air without direct contact with the desiccant [13–20]. The membranes used are permeable to water vapor but impermeable to liquid desiccant. The membrane–desiccant systems have been used in two different configurations. The first configuration employs a membrane desiccant system that dehumidifies the supply air before entering the indoor space [15–18]. In this configuration (first), there are two compact energy exchangers, one for dehumidifying the air and the second for regenerating the liquid desiccant [15,18]. Since simultaneous heating and cooling are required for the liquid desiccant operation cycle, the liquid desiccant membrane system has been integrated with conventional vapor compression reverse cycle forming a hybrid air conditioning system [19]. The results showed that such integrated system has a higher coefficient of performance (COP) compared to the conventional air conditioning system since the cooling coil is operating at a higher temperature and the regeneration of the liquid desiccant utilizes the dissipated condenser heat [19]. Some of the compact energy exchangers that have been studied in literature are Liquid-to-air membrane energy exchanger (LAMEE) [16] and run-around membrane energy exchanger (RAMEE) [17] systems. The semi-permeable membrane allows simultaneous heat and moisture transfer between the air and desiccant solution streams. A RAMEE is comprised of two or more separated liquid-to-air membrane energy exchangers and an aqueous desiccant solution that is pumped in a closed loop between the LAMEE.

The other configuration (second), which has been less referenced in the literature compared to the first one of hybrid air conditioning system, is the direct indoor dehumidification, where a permeable membrane is placed in the indoor space picking up moisture, as it is generated, directly from the indoor air. Even though this configuration has received less attention than the first one, nevertheless it has a promising performance and can have additional advantages.

Direct indoor dehumidification has many advantages over outdoor dehumidification. It may offer better humidity control for the indoor environment during transient latent load changes if the driving force for the dehumidification process (the difference between the vapor pressure in the air and in the desiccant aqueous solution) is properly regulated to minimize transient delays [11,13]. In the configuration where dehumidification is occurring directly in the internal space, the supply air humidity ratio may not need to be decreased below the indoor humidity ratio as it is the case with the first configuration where the supply air humidity ratio is lowered before delivering the conditioned to the space. It should be noted that in the case of indoor dehumidification, the supply air humidity ratio cannot have higher values than the indoor humidity ratio to prevent any possible condensation.

One of the novel configurations that have been used to perform indoor dehumidification is the Heat and Moisture Transfer Panel (HAMP) [11,13,14]. The analysis of the HAMP was mainly focused on its efficiency and performance in handling internal latent and sensible loads; hence it was placed in an open loop cycle where the liquid desiccant was conditioned before it enters to the indoor space [11,13]. Regenerating the liquid desiccant was not included in both studies [11,13].

Even though the literature findings suggest that both internal and external dehumidification configurations have improved efficiency as compared to conventional air conditioning system, the integration with renewable energy of direct indoor dehumidification configuration has not been established yet [18]. As for external dehumidification a recent study has been conducted [21] that covers the subject. Thus the integration of permeable desiccant system (in both configurations) is not covered thoroughly in the literature [18,21]. There is an increased emphasis on utilizing renewable energy sources to decrease the negative economic and environmental outcomes associated with fossil fuels. The second dehumidification configuration, which uses indoor dehumidification, may offer a feasible option for an air conditioning system that can be totally powered by renewable energy. Hence, in the presence of a moderate temperature heat sink for cooling the liquid desiccant in the cycle and available solar energy for regeneration, indoor dehumidification might be an effective system to design and operate. The effectiveness of a solar assisted indoor membrane desiccant dehumidification and cooling system has not been addressed by literature.

This study will consider the feasibility of performing a closed cycle membrane desiccant system for direct indoor dehumidification powered by renewable energy. The performance of the system will be investigated through applying it to a typical internal office space in the city of Beirut. Beirut is a coastal city on the Mediterranean Sea, with a minimum temperature of 7–16 °C during winter, and a maximum temperature of 24–32 °C during summer, and relative humidity that varies between 60% and 80% [22]. Due to the humid warm weather during the summer time, efficient dehumidification is desirable during that period. The proximity to sea water can be used as heat sink [23] and the abundance of solar radiation throughout summer makes the solar-regenerated membrane desiccant system an attractive dehumidification system to implement in Beirut. To achieve the stated objective, a mathematical model of the desiccant membrane system is developed and integrated with the internal space model and solar panel thermal model. The desiccant membrane system model is then validated by experiments. This is followed by a simulated case study using the proposed solar-regenerated membrane desiccant system in Beirut climate to evaluate its feasibility in dehumidifying room air and providing thermal comfort in the space and to compare its performance to conventional HVAC systems. The energy consumption of both systems will be evaluated in order to determine which dehumidification process is more effective and less costly.

2. System description

The proposed dehumidification system is composed of the dehumidification permeable pipes, desiccant regeneration permeable pipes, sensible heat exchangers, regeneration heat exchanger, and parabolic solar collectors. Fig. 1 illustrates the system components. The membrane–desiccant system controls the space relative humidity, while the heat sink source is used to cool the air before it enters to the room.

The piping system is made of solid piping lines except in the regenerator and dehumidifier parts. In those sections the main pipe is divided to many pipes where each is made of a porous material, micro porous polypropylene-commercial name Propore®, which is permeable to water vapor but not liquid. The permeable pipes are put inside the indoor space to absorb the moisture from the air and hence perform direct indoor dehumidification. A similar set of pipes is exposed to the ambient air in order to regenerate the liquid desiccant. The regeneration permeable pipes will not be subjected to direct sunlight-especially UV rays- and they are put in shades in case they are exposed to ambient air [24].

The close loop cycle starts as follows. The cool strong liquid desiccant enters the permeable–membrane pipes at (7) picking the moisture from the indoor space (1) to leave at (2) where it is pumped through a solid piping. The desiccant solution then gets heated from the high temperature desiccant leaving the regenerative membrane (exchanger A) and solar energy stored in the tank (exchanger B). The heated desiccant then enters the regenerator, at (4), i.e. the permeable pipes in contact with ambient air. It then loses the absorbed indoor moisture to the external ambient environment. To ensure that the desiccant does not impose an additional sensible indoor heat load and to increase its ability in picking the indoor moisture, the desiccant will first exchange heat with the cool desiccant solution leaving indoor room (exchanger A), then it will be further cooled through the heat sink (exchanger (C)). After passing through exchanger (C), the desiccant enters the dehumidifier again at (7).

The liquid desiccant needs to be heated (regenerated) in order to expel the moisture it has absorbed from the indoor environment. The energy source required for regeneration in this work is solar energy. The solar irradiance is assumed to be collected through parabolic plate collectors that heat a working fluid, which in turn transfers the heat and stores it in a storage tank.

3. Methodology

The membrane desiccant cycle is modeled and simulated to study its efficiency in dehumidifying indoor space. Steady state and 1-D models for the different cycle subsystems; dehumidification/regeneration pipes and heat exchangers are developed. The liquid desiccant membrane cycle is integrated with the quasi-steady state space model to predict the performance of the proposed system in controlling the space relative humidity.

Following the model development, experimental tests are conducted to validate the mathematical model and its ability in predicting humidity removal from the space. Then the system will be applied to a case study where its performance in Beirut City is evaluated and compared to vapor compression cycles.

4. Mathematical model

4.1. Desiccant membrane system

To predict the performance of the membrane–desiccant system, it will be integrated with an internal space model and parabolic solar collectors. The membrane–desiccant system consists of the desiccant solution within the permeable pipes along with its interaction with the indoor space temperature and humidity. In order to derive a mathematical model for heat and mass transfer across the pipes, the thermo-physical properties of the pipe material should be known, which include the vapor diffusivity and thermal conductivity of Propore®.

4.2. Dehumidifier/regenerator

The mass flow on dry basis, i.e. the desiccant, $CaCl_2$ flow rate per second, is assumed constant in the pipes while the total mass flow rate is variable due to absorption or desorption of liquid water. In the proposed cycle a permeable membrane that separates the two phases, i.e. the liquid desiccant and the air outside, exists. Many models that govern mass and energy transfer are found in literature. Zhang et al. [24–27] has derived an analytical solution for hollow fibers that are used in air dehumidification [24] while Huang et al. [28–31] have performed numerical simulations using 2-D analysis. This paper uses a simplified model following derivations published by Zhang et al. [24], Huang et al. [31], Larson [32], Hemingson et al. [17], Bergero et al. [33] and Fan et al. [34].

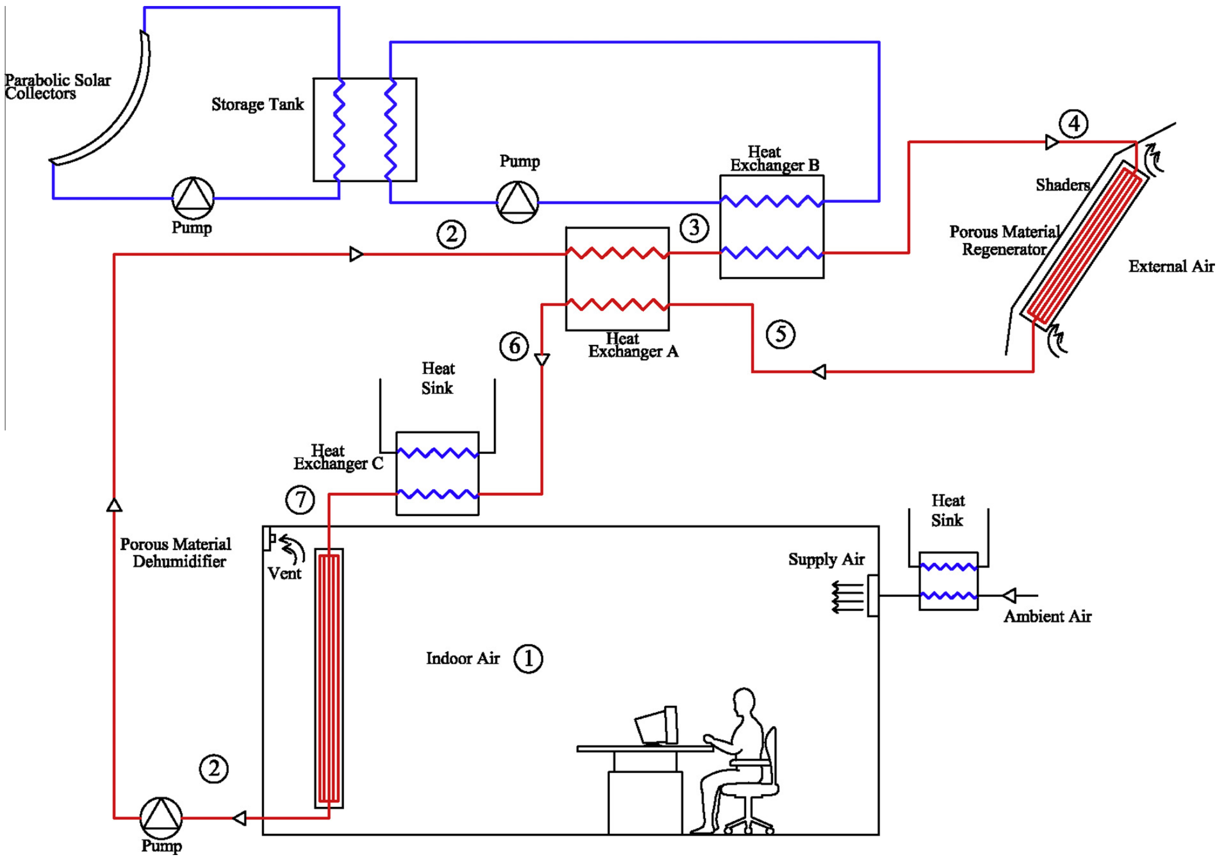

Fig. 1. Schematic of the system.

The mathematical model was derived under the following assumptions: 1-D heat and moisture variation, no energy or mass storage in the pipe membrane, i.e. quasi-steady model, the mechanism of vapor transport in the membrane is only due to diffusion and the axial heat conduction and vapor diffusion in the pipe are neglected. Applying the above assumptions, the energy equation is then given by

$$0 = -m_d \frac{d}{dy}\{h_{solution}(1 + c_{solution})\} + U_c(T_o - T_{solution}) + h_{fg}\rho_a U_m(\omega_0 - \omega^*_{solution}) \quad (1)$$

The first term on the right represents the net convective energy flow and the second term represents sensible energy added to the solution due to difference in temperature between liquid desiccant and the surrounding air temperature. The last term represents the energy added due to the absorption of moisture into the solution. The overall heat transfer coefficient, U_c, per unit length, is represented by

$$U_c = \left\{\frac{1}{2\pi r_o h_{c,o}} + \frac{\ln(r_o/r_i)}{2\pi k} + \frac{1}{2\pi r_i h_{c,i}}\right\}^{-1} \quad (2)$$

Neglecting the solution side mass transfer resistance in the mass transfer process [17], the mass transfer coefficient, U_m, per unit length, is represented by

$$U_m = \left\{\frac{1}{2\pi r_o h_{m,o}} + \frac{\ln(r_o/r_i)}{2\pi D}\right\}^{-1} \quad (3)$$

Some studies have included the solution side mass resistance coefficient [31,34] while others have removed it from the total mass transfer resistance [17]. Hemingson et al. [17] found that neglecting the internal mass transfer resistance will have minimal

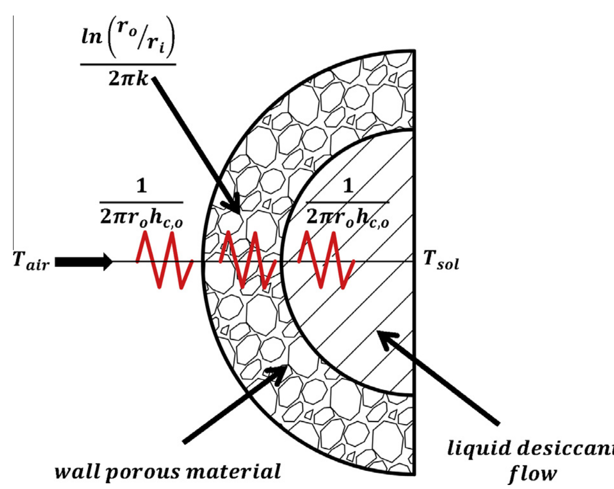

Fig. 2. Thermal resistance model.

effects (about 2%) on mass transfer. Eqs. (2) and (3) couple the membrane properties of the pipe with the flow properties on both sides of the membrane as shown in Fig. 2. The mass convection coefficient is calculated according to the following equation [34]:

$$h_m = h_c \frac{Le^{-\frac{2}{3}}}{c_{p,a}} \quad (4)$$

The species conservation equation for the permeable pipes is

$$0 = -m_d \frac{dc}{dy} + \rho_a U_m(\omega_0 - \omega^*_{solution}) \quad (5)$$

The first term on the right represents the net moisture convective flow and the second term represents the moisture transfer from the surrounding air to the solution in the pipe, across a concentration difference of $(\omega_0 - \omega^*_{solution})$. The humidity ratio in the surrounding air is ω_0 while $\omega^*_{solution}$ is the equilibrium humidity of the liquid desiccant at the solution's temperature and concentration, $T_{solution}$ and $c_{solution}$ respectively.

4.3. Modeling of indoor space

In this study, a model for indoor space is developed following the work done in [35] under the following assumptions: quasi steady state where a steady state model for the room is used with varying sensible and latent loads assuming that the space loads are all internal loads where the thermal and moisture inertial effects are neglected [36,37]. The model assumes that the air is well mixed; hence the average values for temperature and humidity ratio are used to represent the temperature and humidity of the room. The space represents an internal office room in a typical firm in Beirut City. Applying the above assumptions and knowing the flow rate and the conditions of the supplied air, the space energy equation assuming perfect mixing can be written as

$$m_a c_{p,a}(T_{inlet} - T_o) + m_a c_{p,v}(T_{inlet}\omega_{inlet} - T_o\omega_o) + Q = \sum_{i=1}^{n}\int_0^{l_i} U_c(T_o - T_{solution})dy \tag{6}$$

where the first two terms on the left side of the equation represent the convective sensible heat flows, of dry air and water vapor respectively, and the last term represents the space internal load (sensible). The term on the right side of the equation represents the sensible energy transfer with the set of desiccant membrane pipes found in the indoor space. It is integrated over the whole length l of each pipe to take into consideration the variation of temperature in the pipe.

Similarly, the space moisture balance equation can be represented as

$$m_a(\omega_{inlet} - \omega_o) + m_g = \sum_{i=1}^{n}\int_0^{l_i} U_m\rho_a(\omega_o - \omega^*_{solution})dy \tag{7}$$

The two terms on the left side of the equation represent the convective moisture transfer and the internal moisture generation. The right side of the equation represents the moisture exchange with the desiccant membrane piping system.

4.4. Modeling of the solar collector and heat exchangers

The energy required for regeneration of the liquid desiccant is supplied from the solar irradiance. Parabolic solar collectors are used to harvest the solar energy and supply the required heat for the cycle. The model developed in [38] is used in this study where it has been integrated with the other subsystems in the cycle to form the total numerical model which is used in the simulations.

The model for the heat exchangers used in the cycles is adopted from [39]. The effectiveness method is used with effectiveness of 0.85 for all heat exchangers in the liquid desiccant cycle.

5. Numerical method

In order to simulate the effectiveness of the membrane desiccant system in dehumidifying the indoor space, the following input conditions are needed: (1) the dimensions and the physical and thermal properties of the permeable pipes; (2) the internal sensible and latent load profile; (3) the ambient conditions; (4) the supply conditions of the air to the indoor space; and (5) the temperature, mass concentration and the mass flow rate of the desiccant solution entering the indoor space through the permeable pipes. A finite difference method is used to solve for the temperature and concentration variation of the pipes in the room, under steady state assumptions. The dehumidification and regeneration pipes are discretized into 100 elements in order to account for the temperature and concentration variation along the length of the pipe. Simulations were performed with finer grid (125 elements) and it was found that any further increase in the number of elements along the pipe length did not lead to improvement in obtained results on temperature, humidity or liquid desiccant concentration at exit from the space. The average temperature and humidity in the indoor space is calculated using the developed model. The storage tank that couples the solar system and the desiccant system is simulated using transient explicit scheme with lumped temperature model.

The solution flow chart is shown in Fig. 3. Simulations start by setting the input conditions to the cycle. Then using the dehumidifier and the internal space model the room temperature, humidity ratio and the exit temperature and concentration of the dehumidifier are calculated. The dehumidifier model consists of solving simultaneously the heat and mass transfer balance Eqs. (1) and (5) using first order finite differencing scheme at every element in the tube.

To regenerate the desiccant, the regenerator model is used to calculate the required regeneration temperature of the cycle. Using the same model, the exit temperature of the regenerator is also calculated. Knowing the inlet and exit temperatures at the regenerator and dehumidifier, the cooling and heating needs of the desiccant cycle are evaluated through the heat exchanger model. The resulting regeneration energy along with the solar flux during the day, are used as an input to the solar system in order to calculate the storage tank temperature. The simulations of the tank will run for a period of one day.

6. Experimental setup and material selection

To test the regeneration and absorption ability of the permeable membrane used in the study and to validate the theoretical model, an experimental setup was built. The setup was composed of a membrane dehumidifier, membrane regenerator, heat exchanger, and heating tank. The supply air to the dehumidifier and regenerator was supplied from two different environmental chambers.

The pipe material choice is of fundamental importance. The material should be permeable to moisture but not to liquid water. The pipe material chosen in the experimental apparatus is Propore® (Microporous polypropylene membrane) which has high water vapor permeability. This material has been used in previous similar applications [14,32]. As for the desiccant material, Calcium Chloride is chosen in this application because it is one of the most common working fluid in absorption systems [40]. Its moisture absorption capability and low corrosiveness along with its cheap price makes it an attractive choice for such applications. A schematic of the experimental setup showing the regenerator tubes, dehumidifier tubes, heating tank and cooling heat exchanger is shown in Fig. 4.

The dehumidifier and regenerator tubes were enclosed in a rectangular air duct of length 2 m and a cross section of 7 cm × 30 cm with controlled suction fans at the end. Inside the air ducts there were four cylindrical pipes made from Propore® material. The pipes were manufactured through cutting a rectangular piece of Propore® of length 1.36 m and 6.3 cm in width. The rectangular piece is then folded along the width to form a cylinder of diameter 2 ± 0.1 cm and length 1.36 ± 0.01 m. Two metallic sheets were pressed along the top part of the rectangular piece and held together by small clamps in order to give the pipes the cylindrical shape and keep them intact once the liquid desiccant

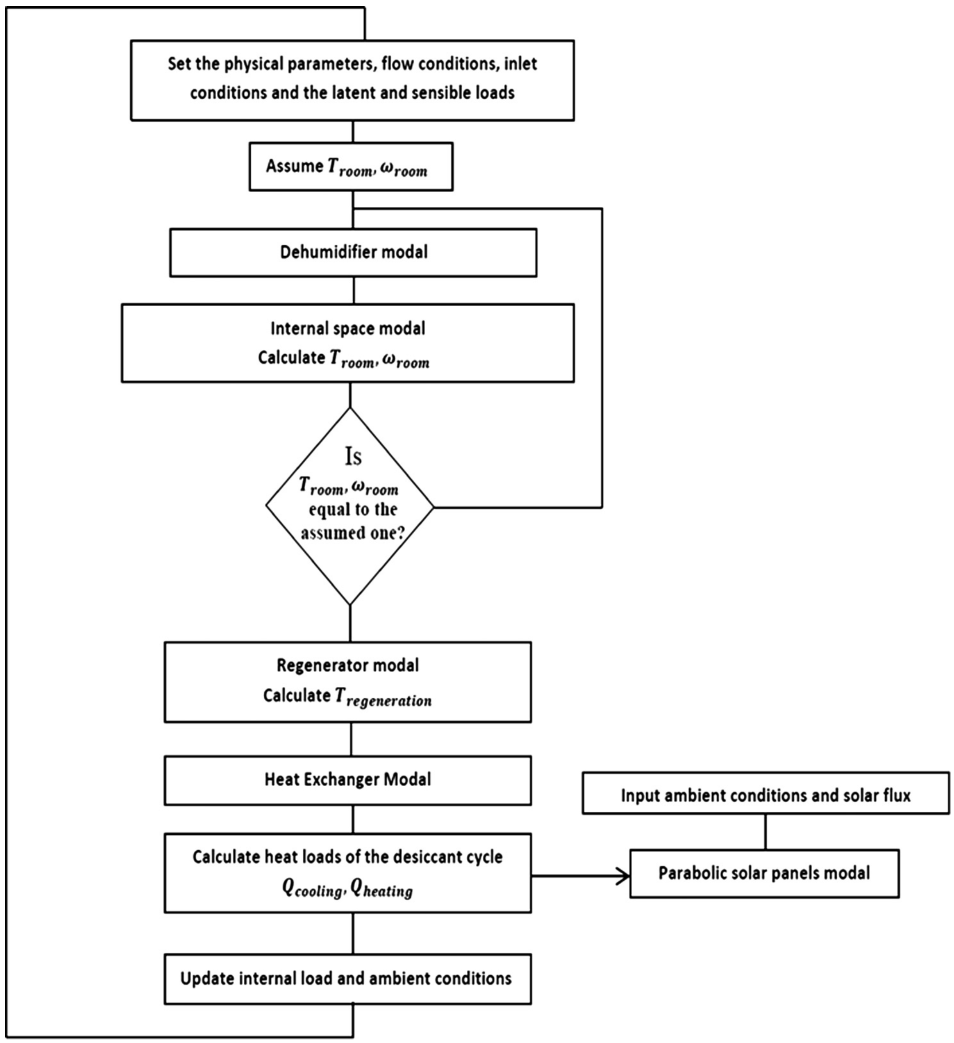

Fig. 3. Simulation flow chart.

flow passes through them, as shown in Fig. 5. The working fluid in the setup was a liquid desiccant solution made of $CaCl_2$ and water with a concentration of 38 ± 1%. The flow rate of the desiccant was set to 69 L/h. The liquid flow was sufficient to fill and completely inflate the pipes giving them their circular shape and minimizing the possible non-uniformity of the pipe diameter. This is necessary since the simplified 1-D model does not account for the possible non-uniformity in the pipe diameter over the length of the 1.36 m long pipe. The desiccant temperature entering the regenerator was controlled through a PID controller and was set at 39 °C with a ±1 °C steady state error from the set value. The controller was applied to the heating tank which has a heating capacity of 2200 Watts and total volume of 6 l. The temperature of the desiccant entering the dehumidifier was controlled through monitoring the flow of chilled water to the heat exchanger. The temperature at the inlet of the dehumidifier was set at 24 °C and measured through a type K thermocouple; the error in the reading is ±0.5 °C.

The air at the inlet of the dehumidifier duct was supplied from an environmental chamber maintained at a mean fixed temperature of 25.8 °C ± 0.3 and mean humidity ratio of 17.45 g_w/kg_a ± 0.65. The inlet air at the regenerator was taken from the lab environment at 24.5 °C ± 0.3 and mean humidity ratio of 12.38 ± 0.54 g_w/kg_a. Sensors at the inlet and exit of the air flow in the dehumidifier and regenerator were added to monitor the properties of the air and hence calculate the mass and heat transfer to it. The sensors used are OMEGA® HX94A Series Humidity/Temperature sensors with relative humidity accuracy of ±2.5% and temperature accuracy of ±0.3 °C. The sensors were connected to a data acquisition system which was used to process the input data of the sensors. The mass flow rate of the air in the dehumidifier/regenerator was calculated through measuring the air velocity with an anemometer, with error of 3% of the reading. The air mass flow rate was set at 1.12 g/s by controlling the speed of the suction fans.

After turning on the fans and the pump and regulating the cooling water valves, the sensors were turned on to take the readings and the testing setup was left to operate for 4 h. The measurements were saved after observing the temperature and humidity ratio at the exit of the dehumidifier and regenerator stabilized (fluctuations of less than 2% and 5% of the instantaneous measured value relative to the average measured values over one hour of the temperature and the humidity ratio, respectively). The measurements taken for the inlet and exit conditions of the regenerator and dehumidifier are shown in Fig. 6 and Fig. 7 respectively.

In order to check the moisture balance of the setup, i.e. the moisture desorbed by the regenerator is equal to that absorbed by the dehumidifier; a moisture balance was made on both components. The moisture balance was performed using average values for the inlet and exit conditions of the regenerator and dehumidifier. The rate of mass absorbed/desorbed is calculated using the following mass balance:

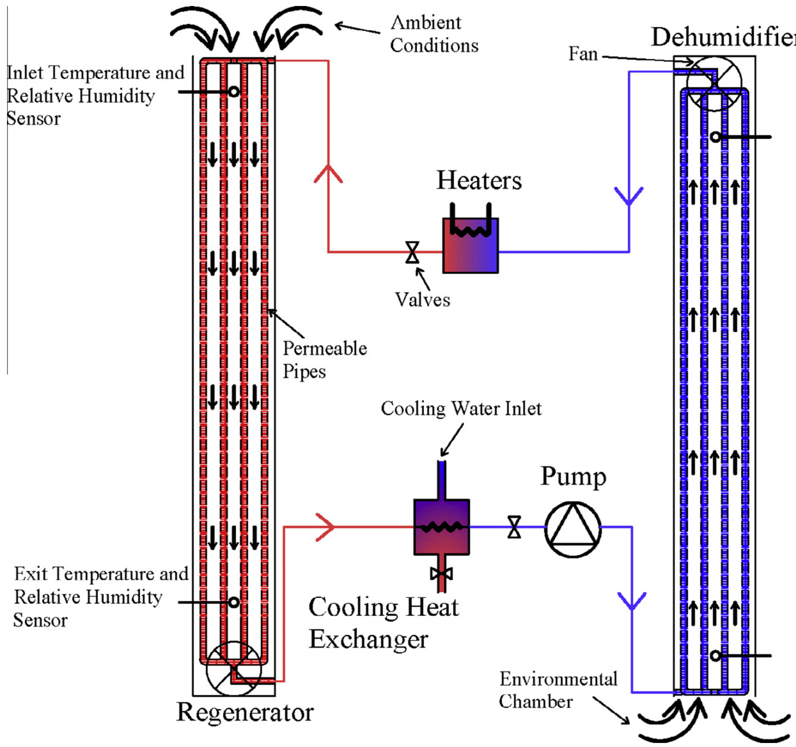

Fig. 4. Schematic of the experimental setup.

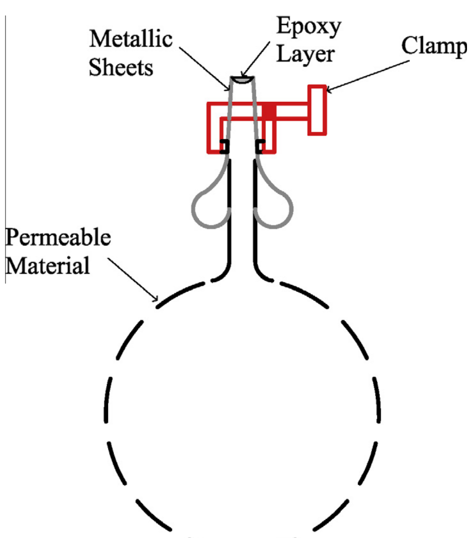

Fig. 5. Pipe Assembly.

$$m_g = m_a(\omega_{inlet} - \omega_{outlet}) \tag{8}$$

The rate of moisture absorption by the dehumidifier is found to be 2.37×10^{-3} g/s while that of the regenerator was 2.6×10^{-3} g/s, with an error of $\pm 3.36 \times 10^{-5}$ g/s in estimation of the mass flow rate from velocity measurements. This error is 9.7% of the moisture value desorbed in the dehumidifier. This error is within the total experimental setup accuracy.

At the end of the experiment, the concentration in the tanks did not change and remained at the initial value of 38%, as measured by the titration technique HACH 8225 for chloride and HACH 8226 for calcium hardness [41].

The energy balance of the system was done by taking a control volume over the whole system. The energy inputs were the enthalpy of air entering the dehumidifier and regenerator and the heat input through the heaters. Whereas, the energy outputs were energy through the cooling heat exchanger and enthalpy of the air leaving the regenerator and dehumidifier. Eq. (9) is used to evaluate the total energy balance of the system.

$$\Delta E = E_{inlet} - E_{outlet} \tag{9}$$

The difference between inlet and outlet energy in the cycle was less than 6.2 W. The error in the estimation of energy input and energy output is ±12 W based on heater input error, air flow error, and temperature measurement error. This error is less than 6% of the energy input of the heater at 2200 W.

7. Results and discussions

7.1. Model validation

The integrated model of liquid desiccant membrane dehumidification system was simulated for the geometric and physical parameters of the experiment while using the experimentally measured average inlet conditions to the regenerator and dehumidifier as inputs to the model. To simulate the mathematical model, the membrane material properties were taken as 5.2×10^{-7} m^2/s for the material vapor diffusivity and 0.34 W/m K for the thermal conductivity [42]. The external convection coefficient of the pipe wall in other studies [13] used natural convection correlations over vertical wall for vertical membrane configuration. For our experiment, the pipes were placed horizontally in the duct and the Reynolds number of the air flow based on duct hydraulic diameter was around 70 which was the case of laminar developing forced convection flow [37]. The average calculated convection coefficient used in the model for the conditions of the experiment was 3.1 W/m K. It should be noted that the laminar forced convection may not be the case in indoor air conditioning applications where natural convection usually prevails. However, given the experimental setup constraints, the laminar forced convection

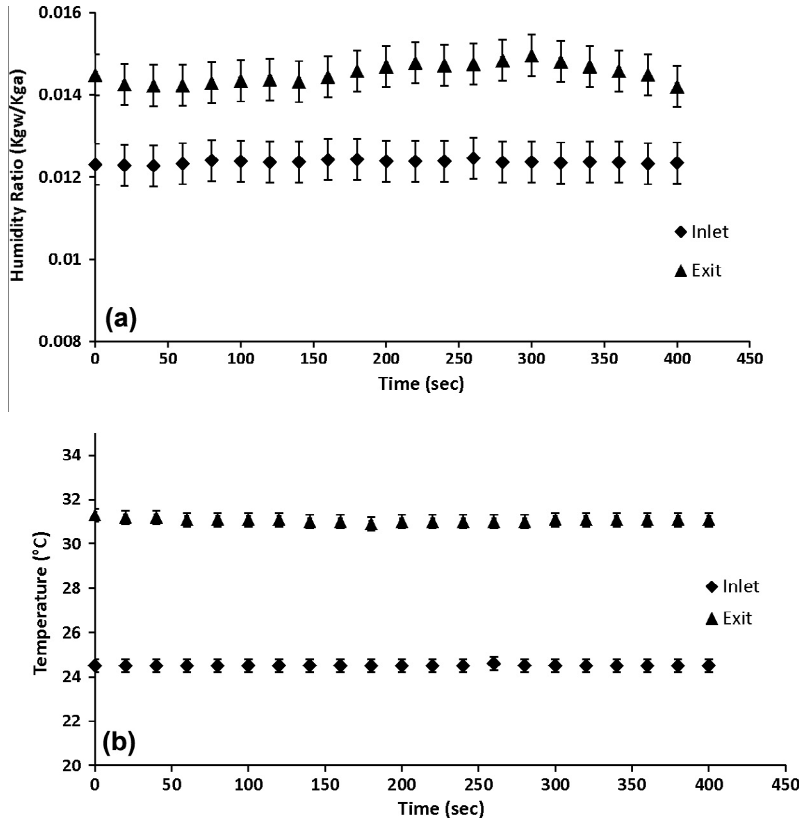

Fig. 6. The inlet and exit conditions to the regenerator; (a) humidity ratio and (b) temperature.

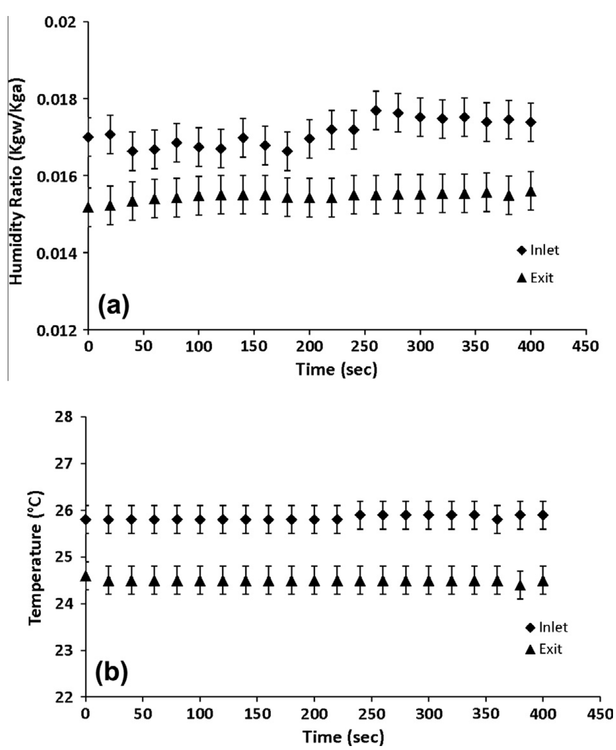

Fig. 7. The inlet and exit conditions to the dehumidifier; (a) humidity ratio and (b) temperature.

assumption is valid. Nevertheless the value of the heat convection coefficient used for natural convection was close to the value used in this study [42].

The predictions of the mathematical model and the actual experimental measurements of exit temperature and humidity of the humidifier and regenerator are summarized in Table 1. The experimental conditions are calculated as the average values of the measured quantity over the last hour. The uncertainty in the measurements takes into consideration the fluctuations of the measured value around the average (standard deviation) and the uncertainty in the measuring sensor. As shown in Table 1, the model was able to predict the exit conditions. The error in predicting the temperature was 6.5% in the dehumidifier and 2% in the regenerator. As for the humidity ratio, the error was 5.4% in the dehumidifier and 4% in the regenerator. The error in predicting the humidity ratio in both the dehumidifier and regenerator were comparable while the temperature prediction was slightly better for the regenerator as compared to the dehumidifier. In literature, the disagreement between measured data and model predictions was more for the regenerator [43]. For a simplified model, the difference between the expected and the actual is acceptable.

7.2. Case study

In order to test the efficiency of the membrane desiccant cycle, it will be applied to an internal office space, of dimensions 3 m × 6 m × 7 m, in the city of Beirut (see Fig. 1). As mentioned earlier, Beirut is a coastal city; hence sea water at 17 °C can be used as a heat sink to supply the required cooling loads [22].

The office under study has a typical latent and sensible load profile shown in Table 2 [44]. The membrane desiccant system is used as the primary system to lower the humidity level in the office. The dehumidification pipes of the system are assumed to be installed in a vertical manner on one of the room walls. To ensure efficient dehumidification, the length of the pipes is equal to the room height, which is 3 m. The total number of pipes used is 190, covering the wall area, each with an outer diameter of

Table 1
Comparison between experimental and theoretical.

	Inlet conditions		Exit theoretical		Exit experimental	
	Temperature (°C)	Humidity ratio (g_w/kg_a)	Temperature (°C)	Humidity ratio (g_w/kg_a)	Temperature (°C)	Humidity ratio (g_w/kg_a)
Dehumidifier	25.8 ± 0.3	17.4 ± 0.6	26.1 ± 0.1	14.5 ± 0.08	24.6 ± 0.3	15.3 ± 0.6
Regenerator	24.5 ± 0.3	12.3 ± 0.5	30.54 ± 0.1	15.28 ± 0.08	31.1 ± 0.3	14.7 ± 0.6

Table 2
Internal loads and ambient conditions.

	Internal sensible load (W)	Internal latent load (W)	Supply air flow rate (kg/s)	Ambient temperature (°C)	Ambient humidity ratio (g_w/kg_a)	Solar flux (W)
8:00–9:00	987	128	0.16	29	17.02	512
9:00–10:00	987	128	0.16	30	18.06	653
10:00–11:00	987	128	0.16	30	18.06	754
11:00–12:00	1554	256	0.22	31	19.15	798
12:00–13:00	1554	256	0.22	31	19.15	780
13:00–14:00	1554	256	0.22	30	18.06	701
2:00–3:00	1392	220	0.20	31	19.15	574
3:00–4:00	1392	220	0.20	31	19.15	419
4:00–5:00	1392	220	0.20	31	19.15	256

2.3 cm. The large number of dehumidification tubes considered is to ensure that there is sufficient mass transfer area between the liquid desiccant in the tubes and the room air. A diameter of 2.3 cm for the tubes was selected to insure that the whole wall area is covered with tubes with small distance between them ignoring any possible maldistribution that might occur due to irregularity in both the pipe diameter over the 3 m individual pipe length and the amount of desiccant entering the pipe.

The indoor space is conditioned by 100% fresh air. Using the heat sink at 17 °C, the fresh air temperature is lowered from the external ambient temperature to a temperature of 18 °C. The selection of the low heat sink temperature was to avoid the need additional cooling to the supply air to the room or increase the supply flow rate which would bring more saturated air to the room increasing moisture removal load. The target is to have a system that is 100% renewable. The system would perfectly work for lower heat sink temperatures if it is working for 17 °C. If the dew point temperature of the ambient air is higher than 18 °C (which is typical for a summer day in Beirut City), the supply air will enter at 100% relative humidity and 12.93 g_w/kg_a humidity ratio. The corresponding supply air flow rates, needed to maintain room temperature around 24 °C, are shown in Table 2. As for the liquid desiccant entering the room through the pipes, a dehumidification temperature of 23 °C and concentration of 40% is chosen ensuring dehumidification [45]. The desiccant mass flow rate is set at 3.6 kg/hr per pipe [46,33], to minimize the heat input to the cycle and at the same time to ensure that no sensible load is added to the indoor space due to the heating of the desiccant solution associated with the release of absorption energy upon moisture removal. As for the regeneration tubes, their number and diameter is equal to that of the dehumidification pipes placed in the indoor area, i.e. 190 tube and 2.3 cm respectively. Their length however is reduced from 3 m to 1 m to prevent excessive drop in the desiccant temperature upon interacting with the ambient air, due to the low desiccant flow rate in the tubes.

The regeneration thermal energy required by the membrane system is assumed to be supplied through the use of parabolic solar panels and a storage tank [23,38]. The parabolic solar panels will be sized according to the thermal energy consumption required by the desiccant to raise its temperature to the regeneration temperature, with the provision that the area occupied by the solar concentrators does not cover more than 40% of the roof area.

The model is simulated for a representative day in August (15th of the month), with the ambient conditions shown in Table 2. To evaluate the performance of the system and its efficiency in removing humidity from indoor space, two cases are considered, case (A) the room model with the membrane desiccant system and case (B) the room model without the desiccant system. The hourly variation of the room temperature, humidity ratio and relative humidity for both cases are shown in Fig. 8, Fig. 9 and Fig. 10, respectively, whereas the hourly thermal energy needed for the regeneration of the desiccant is shown in Fig. 11.

7.2.1. Membrane desiccant system performance

In the absence of the membrane system (case A), the conditioned air was able to maintain a good comfort temperature but not a good relative humidity. The indoor air temperature for case (A) was on average 24.2 °C ranging between 23.8 °C and 24.5 °C and reaching a peak value at noon time in accordance with the sensible load, as shown in Fig. 8. The average value of the humidity ratio was 13.38 g_w/kg_a, which was higher than the supply air humidity ratio of 12.93 g_w/kg_a due to the latent load in the room. The humidity ratio reached a peak of 13.45 g_w/kg_a at noon hour, when the latent load was the highest as shown in Fig. 9. The relative humidity achieved in case (A) was on average 70.2%, where its highest value was 71.8% during the morning, due to the low temperature of the indoor space and then it decreased throughout the day due to the increase in the temperature of indoor air, as shown in Fig. 10.

In the presence of the solar regenerated membrane desiccant system (Case B), the room temperature slightly increased throughout the day by an average value of 0.25 °C, as was shown in Fig. 8.

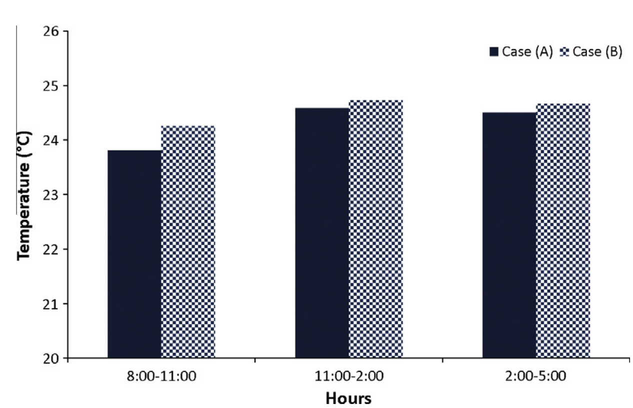

Fig. 8. Indoor temperature variation; case (A) without the membrane system, case (B) with the membrane system.

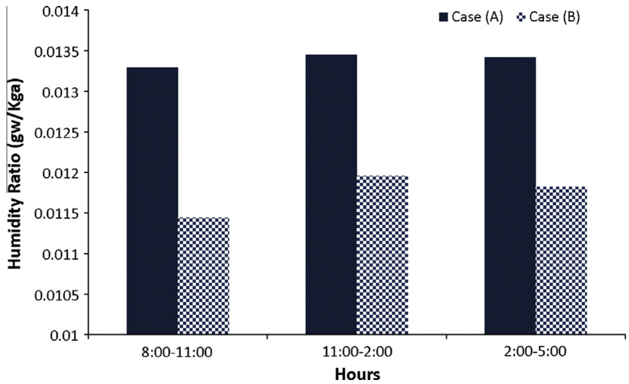

Fig. 9. Indoor humidity ratio variation; case (A) without the membrane system, case (B) with the membrane system.

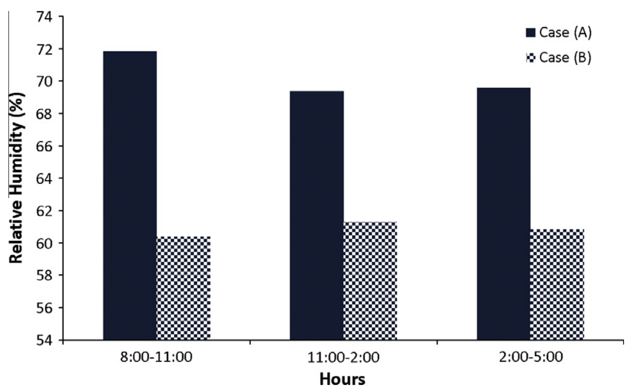

Fig. 10. Indoor relative humidity variation; case (A) without the membrane system, case (B) with the membrane system.

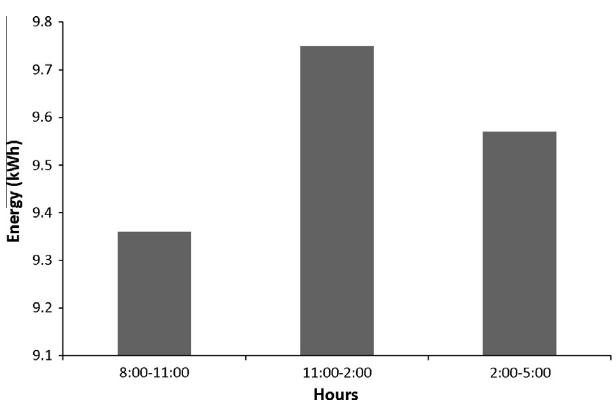

Fig. 11. Thermal energy consumption of the membrane desiccant system with respect to time.

The slight increase in the room temperature is due to vapor absorption along the length of the pipes. The absorption energy associated with moisture removal increased the liquid desiccant temperature in the tubes which in turn heated slightly the indoor air. However, this effect has minimal impact on the indoor space temperature where the increase is only 1% of the room temperature. As for the humidity ratio of the indoor air of case (B), it was consistently lower than that of case (A) (see Fig. 9). The difference between the average humidity ratio of the liquid desiccant, $\omega^*_{solution}$ of 7.7 g_w/kg_a, and the room air is the driving potential for moisture absorption through the permeable membrane. The average humidity ratio of the indoor air was 11.7 g_w/kg_a where it ranged from 11.44 g_w/kg_a to a peak value of 11.95 g_w/kg_a during midday. The jump in the value of the room humidity ratio is attributed to two factors. The first is the increase of the latent load during midday and the second is the increase of the flow rate of the humid supply air during midday, which was necessary to maintain an indoor temperature around 24 °C. The indoor air relative humidity in case (B) was on average 60% as compared to a value of 70% for case (A) (see Fig. 10). Due to the slight increase in the room temperature and due to the substantial reduction in the room humidity ratio, the membrane system has helped in stabilizing the relative humidity value around 60% throughout the day. The indoor humidity ratio, relative humidity and temperature achieved in the presence of the membrane system (Case B) were within the acceptable thermal comfort zone as set by ASHRAE Standard 55 [1,47], which recommends a strict upper limit of 0.012 kg_w/kg_a for humidity ratio, a relative humidity between 56% and 67% and a temperature between 24 and 28 °C during the summer.

The thermal energy consumption of the membrane desiccant system was low during the beginning of the day, it peaked during mid-day and then it decreased towards the end, as shown in Fig. 11. This is in accordance with the ambient humidity ratio variation. As the humidity of the ambient increases, the regeneration temperature of the desiccant increased in order to raise the desiccant humidity ratio, $\omega^*_{solution}$.

Due to the low flow rate of the desiccant used, the system generally consumed relatively low thermal energy (around 3.18 kW as a mean value).

7.2.2. Economic analysis of the membrane system vs. Conventional vapor compression system

To estimate the economic feasibility and energy efficiency of the membrane desiccant system, it will be compared to a conventional vapor compression system (has been in operation for over 100 years) that can attain the same indoor conditions (temperature and relative humidity within the thermal comfort zone) as that of the membrane system. The comparison is done over a period of five month consisting of May, June, July, August and September, which represent the most humid months of Beirut City and which require efficient dehumidification.

The vapor compression cycle is assumed to have a coefficient of performance (COP) of 3. It first subcools the supply air to reach the required humidity ratio, and then through the use of an electric heating coil, the supply air is reheated to the appropriate supply temperature. Gas combustors could have been used to reheat the air following the vapor compression dehumidification; however in Lebanon gas combustors are usually used in buildings and not in small office spaces.

For the case study office space considered in August and simulated in Section 7.2.2, the electric energy required for subcooling and the reheat energy required during one day of operation are shown in Table 3. A total daily electric energy consumption of 8 kW h is consumed by the vapor compression cycle in the reheat–subcool process. This amount will not change throughout the considered period of five month since the loads are mostly internal and the supply conditions to the room are the same. The average ambient temperatures during the considered months is above 24 °C and the dew temperature of the air is on average higher than 18 °C, thus the supply conditions to the room do not change and hence the amount of 8 kW h remains the same. Over a period of five month the total electric energy consumption will be 1372.5 kW h.

As for the membrane system, the ambient conditions are varying every month, and hence the regeneration temperature of the desiccant will vary accordingly given that the membrane desiccant system is desorbing the moisture to the ambient environment. To estimate the regeneration energy of the desiccant, a representative day was taken for each month and the model was simulated for

Table 3
Energy loads for the membrane desiccant system and conventional system.

	Subcool energy (kW h)	Electric energy required for the subcool (kW h)	Reheat electric energy (kW h)	Total electric energy (kW h)
8:00–11:00	3.67	1.223	1.39	2.613
11:00–2:00	4.061	1.354	1.37	2.724
2:00–5:00	3.96	1.32	1.343	2.663
Total energy (kWh/day)	11.691	3.897	4.103	8.00

that day [23,48]. The thermal energy requirement for each month is shown in Fig. 12. The thermal energy consumption increases in accordance with the months of highest humidity ratio. As the ambient humidity ratio increases, the regeneration temperature of the desiccant increases and hence the thermal energy requirement of the cycle increases. Having established the thermal load of the membrane desiccant system, the parabolic solar panels and the storage tank can be sized accordingly [23]. A total of 4.8 m × 1.2 m parabolic collectors along with a 1 m^3 storage tank can supply the required thermal energy of the system, given the solar flux profile shown in Table 2. The total surface area of the solar panels and the storage tank cover an area that does not exceed 20% of the roof surface area. Thus the solar system supplies the total heat required without any additional heat sources. The solar fraction, which is the ratio of the heat supplied to the cycle to the heat of the solar energy supplied to the tank, varies from 0.84 in the morning to 0.74 during midday to 1.33 during after noon. The reason for the high solar fraction in the afternoon is that the cycle withdraws heat more that the solar flux supplies heat to the storage tank, due to the fact that the solar flux intensity decreases in the afternoon. The high solar flux during the morning hours and midday compensates for this shortage in flux in the afternoon. An average solar fraction of 0.97 is obtained for a single day in August (August 15).

The aim of the current economic analysis is to determine the payback period using present worth analysis and to obtain the return on the investment in the cost of the membrane system and the parabolic solar collectors. The cost of installing the membrane system is compared to the cost of installing the vapor compression cycle in addition to the cost of electric energy consumed every year. The installation and operating cost of the fan and pump will not be considered in the analysis since they are used in both systems.

The cost of the membrane system includes the initial costs of the dehumidification/regeneration pipes and the parabolic solar panels. The total length of parabolic collectors required to supply the monthly regeneration energy of the membrane desiccant is 4.8 m with a width of 1.2 m. The estimated cost of the parabolic collectors is $2000 [23], where a single module of specifications shown in Table 4 costs. As for the membrane itself, the material used, which is Propore®, costs $5/$m^2$ [32], for a total of 80 m^2 of Propore, the cost is $400. The cost of installation and fabrication

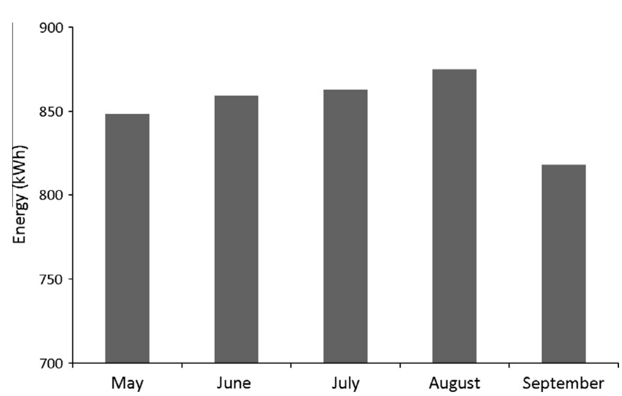

Fig. 12. Monthly thermal consumption of the membrane desiccant cycle.

Table 4
Module specifications of the parabolic solar collector.

Design parameter	Value
Tank specifications	
Tank volume	1 m^3
Tank total surface area	5.545 m^2
Loss coefficient of tank	0.5 W/m^2 k
Parabolic solar module specifications	
Collector tube diameter	0.06 m
Transparent cover tube diameter	0.09 m
Flow rate of water in collector	0.0535 kg/s
Width of the collectors	1.2 m
Length of the collectors	2.4 m

of the membrane pipes is estimated as $500. Therefore the total cost of the membrane–desiccant system is $2900.

Considering a commercially available vapor compression system, the initial installation cost is estimated as $800, whereas the cost of electricity in Beirut City is estimated as 0.19 $/kW h. Therefore the cost of electricity consumption by the vapor compression cycle over the operational period of 5 month per year is calculated to be $261.

In order to determine the present worth value, *P*, of both systems, we us the following expressions at discount rate *d*:

$$P = A_0 \frac{1-\left(\frac{1+i}{1+d}\right)^n}{d-i} \quad i \neq \mathrm{d} \tag{10a}$$

$$P = A_0 \frac{n}{1+d} \quad i = \mathrm{d} \tag{10b}$$

In Eqs. (10a) and (10b), *n* the number of years and *i* is the annual rate at which electricity costs are increasing. Using a discount rate of 2% and assuming an annual rate of electricity price increase as 3%, the payback back period after which the initial investment in the solar collectors [49] and the membrane system is returned to the costumer is 7 years and 8 month.

This is a relatively long payback period. It can be justified that the system is operating for a period of 5 month per year, as compared to other locations in the globe which need dehumidification throughout the year. Other membrane systems that have been studied in literature have a payback period of 4–6 years [45].

8. Conclusions

In this study, the performance and feasibility of a membrane desiccant system integrated with solar energy has been evaluated. A theoretical model has been proposed to integrate the indoor room model with the membrane desiccant system and the parabolic solar collectors. Experiments were performed to validate the theoretical model. The predictions of the theoretical model were in good agreement with the experimental findings. After the validation, the system was applied to a test case for a typical internal office space in Beirut City. The results showed that the system can achieve indoor thermal comfort with minimal effects on room temperature. A drop of 10% of indoor relative humidity was observed when the system was installed. The economic cost of the membrane desiccant system was then compared to a conventional vapor compression cycle that can achieve the same indoor conditions as the desiccant system, in the presence of a heat sink. The cost of the vapor compression cycle in addition to the electricity consumption each year was compared to the initial cost of the solar panels and the membrane system. The payback period to return the initial cost of the investment was estimated, using present worth analysis, and was found to be 7 years and 8 month.

Future research will be focused on the performance of the permeable pipes in removing the latent loads where optimization techniques can be used to set the design parameters of the permeable membrane cycle so as to achieve best dehumidification with minimal thermal and cooling loads.

Acknowledgements

The authors would like to thank the Lebanese National Council for Scientific Research (CNRS) for their financial support. The help of Bashir El Fil, Rami Bitar, Karim Moukalled and Roy Fattouh in setting up and performing experiments is highly acknowledged.

References

[1] Yang L, Yan H, Lam JC. Thermal comfort and building energy consumption implications – a review. Appl Energy 2014;115:164–73.
[2] Ghali K, Katanani O, Al-Hindi M. Modeling of the effect of hygroscopic curtains on relative humidity for spaces air conditioned by DX split air conditioning system. Energ Buildings 2011;43:2093–100.
[3] Straube J. Moisture in buildings. ASHRAE J 2002:15–9. January.
[4] Bahman A, Rosario L, Rahman MM. Analysis of energy savings in a supermarket refrigeration/HVAC system. Appl Energy 2012;98:11–21.
[5] Xiao F, Ge G, Niu X. Control performance of a dedicated outdoor air system adopting liquid desiccant dehumidification. Appl Energy 2011;88:143–9.
[6] Wang X, Cai W, Lu J, Sun Y, Ding X. A hybrid dehumidifier model for real-time performance monitoring, control and optimization in liquid desiccant dehumidification system. Appl Energy 2013;111:449–55.
[7] Li X, Zhang X, Quan S. Single-stage and double-stage photovoltaic driven regeneration for liquid desiccant cooling system. Appl Energy 2011;88:4908–17.
[8] Huang S, Yang M. Longitudinal fluid flow and heat transfer between an elliptical hollow fiber membrane tube bank used for air humidification. Appl Energy 2013;112:75–82.
[9] Mohammad AT, Bin Mat S, Sulaiman MY, Sopian K, Al-abidi AA. Historical review of liquid desiccant evaporation cooling technology. Energ Buildings 2013;67:22–33.
[10] Wang N, Zhang J, Xia X. Desiccant wheel thermal performance modeling for indoor humidity optimal control. Appl Energy 2013;112:999–1005.
[11] Fauchoux M, Bansal M, Talukdar P, Simonson CJ, Torvi D. Testing and modeling of a novel ceiling panel for maintaining space relative humidity by moisture transfer. Int J Heat Mass Transf 2010;53:3961–8.
[12] Studak JW, Peterson JL. A preliminary evaluation of alternative liquid desiccants for a hybrid desiccant air conditioner. In: Proceedings of the fifth symposium on improving building systems in hot and humid climates; 1988.
[13] Eldeeb R, Fauchoux M, Simonson CJ. Applicability of a heat and moisture transfer panel (HAMP) for maintaining space relative humidity in an office building using TRNSYS. Energ Buildings 2013;66:338–45.
[14] Fauchoux MT, Simonson CJ, Torvi D. Tests of a novel ceiling panel for maintaining space relative humidity by moisture transfer from an aqueous salt solution. ASTM Int 2009;6(4):1–10.
[15] Mahmud K, Mahmood GI, Simonson CJ, Besant RW. Performance testing of a counter-cross-flow run-around membrane energy exchanger (RAMEE) system for HVAC applications. Energ Buildings 2010;42:1139–47.
[16] Moghaddam DG, LePoudre P, Besant RW, Simonson CJ. Steady-state performance of a small-scale liquid-to-air membrane energy exchanger for different heat and mass transfer directions, and liquid desiccant types and concentrations: experimental and numerical data. J Heat Transf 2013;135.
[17] Hemingson HB, Simonson CJ, Besant RW. Steady-state performance of a run-around membrane energy exchanger (RAMEE) for a range of outdoor air conditions. Int J Heat Mass Transf 2011;54:1814–24.
[18] Abdel-Salam MRH, Fauchoux M, Ge G, Besant RW, Simonson CJ. Expected energy and economic benefits, and environmental impacts for liquid-to-air membrane energy exchangers (LAMEEs) in HVAC systems: a review. Appl Energy 2014;127:202–18.
[19] Bergero S, Chiari A. Performance analysis of a liquid desiccant and membrane contactor hybrid air-conditioning system. Energ Buildings 2010; 42:1976–86.
[20] Moghaddam DG, Besant RW, Simonson CJ. Solution-side effectiveness for a liquid-to-air membrane energy exchanger used as a dehumidifier/regenerator. Appl Energy 2014;113:872–82.
[21] Abdel-Salam AH, Ge G, Simonson CJ. Thermo-economic performance of a solar membrane liquid desiccant air conditioning system. Sol Energy 2014;102:56–73.
[22] UNDP. UNDP passive climate and comfort design strategies for Lebanon; 2005.
[23] Audah N, Ghaddar N, Ghali K. Optimized solar-powered liquid desiccant system to supply building fresh water and cooling needs. Appl Energy 2011;88:3726–36.
[24] Zhang LZ. An analytical solution to heat and mass transfer in hollow fiber membrane contactors for liquid desiccant air dehumidification. ASME J Heat Transf 2011:092001–8.
[25] Zhang LZ. Coupled heat and mass transfer in an application-scale cross-flow hollow fiber membrane module for air humidification. Int J Heat Mass Transf 2012;55:5861–9.
[26] Zhang LZ, Huang SM, Pei LX. Conjugate heat and mass transfer in a cross-flow hollow fiber membrane contactor for liquid desiccant air dehumidification. Int J Heat Mass Transf 2012;55:8061–72.
[27] Zhang LZ, Zhang N. A heat pump driven and hollow fiber membrane-based liquid desiccant air dehumidification system. Energy 2014;65:441–51.
[28] Huang SM, Yang M, Chen S. Effects of the random distributions on the longitudinal transport phenomena between an elliptical hollow fiber membrane bundle. J Membr Sci 2014;471:362–71.
[29] Huang SM, Yang M, Yang Y, Yang X. Fluid flow and heat transfer across an elliptical hollow fiber membrane tube bank for air humidification. Int J Therm Sci 2014;73:28–37.
[30] Huang SM, Qina FGF, Yang M, Yang X, Zhong WF. Heat and mass transfer deteriorations in an elliptical hollow fiber membrane tube bank for liquid desiccant air dehumidification. Appl Therm Eng 2013;57:90–8.
[31] Huang SM, Yang M, Yang X. Performance analysis of a quasi-counter flow parallel-plate membrane contactor used for liquid desiccant air dehumidification. Appl Therm Eng 2014;63:323–32.
[32] Larson MD. The performance of membranes in a newly proposed runaround heat and moisture exchanger. Master Thesis, University of Saskatchewan; 2006.
[33] Bergero S, Chiari A. Experimental and theoretical analysis of air, humidification/dehumidification process using hydrophobic capillary contractors. Appl Therm Eng 2001;21:1119–35.
[34] Fan H, Besant RW, Simonson CJ, Shang W. Performance of a run-around system for hvac heat and moisture transfer applications using cross-flow plate exchangers coupled with aqueous Lithium Bromide. HVAC R Res 2006;12:13–36.
[35] Yassine B, Ghali K, Ghaddar N, Srour I, Chehab G. A numerical modeling approach to evaluate energy-efficient mechanical. Energ Buildings 2012;55:618–30.
[36] Zhang LZ, Niu JL. Indoor humidity behaviors associated with decoupled cooling in hot and humid climates. Build Environ 2003;38(1):99–107.
[37] Niu JL, Zhang LZ, Zuo HG. Energy savings potential of chilled-ceiling combined with desiccant cooling in hot and humid climates. Energ Buildings 2002;34(5):487–95.
[38] Duffie JA, Beckman W. Solar engineering of thermal processes. 2nd ed. USA: John Wiley & Sons, INC.; 1980.
[39] Incropera FP, Dewitt DP, Bergman TL, Lavine AS. Fundamentals of heat and mass transfer. 6th ed. USA: John Wiley & Sons; 2007.
[40] Conde MR. Properties of aqueous solutions of lithium and calcium chloride: formulations for use in air conditioning equipment design. Int J Therm Sci 2004;43:367–82.
[41] HACH water analysis handbook procedures. HACH Company. 5th ed. Colorado, USA: Loveland; 2008.
[42] Vashistha V, Talukdar P. Numerical studies for performance evaluation of a permeable ceiling panel for regulation of indoor humidity. Energ Buildings 2013;62:158–65.
[43] Gaoming GE, Moghaddam DG, Abdel-Salam AH, Besant RW, Simonson CJ. Comparison of experimental data and a model for heat and mass transfer performance of a liquid-to-air membrane energy exchanger (LAMEE) when used for air dehumidification and salt solution regeneration. Int J Heat Mass Transf 2014;68:119–31.
[44] Hourani ME, Ghali K, Ghaddar N. Effective desiccant dehumidification system with two-stage evaporative cooling for hot and humid climates. Energ Buildings 2014;68:329–38.
[45] Abdel-Salam AH, Simonson CJ. Annual evaluation of energy, environmental and economic performances of a membrane liquid desiccant air conditioning system with/without ERV. Appl Energy 2014;116:134–48.
[46] Rattner AS, Nagavarapu AK, Garimella S, Fuller, Thomas F. Modeling of a flat plate membrane-distillation system for liquid desiccant regeneration in air-conditioning applications. Int J Heat Mass Transf 2011;54:3650–60.
[47] Turner SC. What's new in ASHRAE's standard on comfort. ASHRAE; 2011.
[48] Ghaddar N, Bsat A. Energy conservation of residential buildings in Beirut. Int J Energy Res 1998;32(2):523–46.
[49] Ghaddar N, Ghali K, Najm A. Use of desiccant dehumidification to improve energy utilization in air-conditioning systems. Int J Energy Res 2003;27:1317–38.